

Searching for ultralight bosons within spin measurements of a population of binary black hole mergers

Ken K. Y. Ng,^{1,*} Otto A. Hannuksela,^{2,3,4,†} Salvatore Vitale,¹ and Tjonnie G. F. Li⁴

¹*LIGO Lab, Department of Physics, and Kavli Institute for Astrophysics and Space Research, Massachusetts Institute of Technology, 77 Massachusetts Avenue, Cambridge MA 02139, USA*

²*Nikhef – National Institute for Subatomic Physics, Science Park, 1098 XG Amsterdam, The Netherlands*

³*Department of Physics, Utrecht University, Princetonplein 1, 3584 CC Utrecht, The Netherlands*

⁴*Department of Physics, The Chinese University of Hong Kong, Shatin, NT, Hong Kong*

(Dated: March 6, 2022)

Ultralight bosons can form clouds around rotating black holes if their Compton wavelength is comparable to the black hole size. The boson cloud spins down the black hole through a process called superradiance, lowering the black hole spin to a characteristic value. It has been suggested that spin measurements of the black holes detected by ground-based gravitational-wave detectors can be used to constrain the mass of ultralight bosons. Unfortunately, a measurement of the *individual* black hole spins is often uncertain, resulting in inconclusive results. Instead, we use hierarchical Bayesian inference to *combine* information from multiple gravitational-wave sources and obtain stronger constraints. We show that hundreds of high signal-to-noise ratio gravitational-wave detections are enough to exclude (confirm) the existence of non-interacting bosons in the mass range $[10^{-13}, 3 \times 10^{-12}]$ eV ($[10^{-13}, 10^{-12}]$ eV). The precise number depends on the distribution of black hole spins at formation and the mass of the boson. From the few uninformative spin measurements of binary black hole mergers detected by LIGO and Virgo in their first two observing runs, we cannot draw statistically significant conclusions.

I. INTRODUCTION

Ultralight bosons with masses $\lesssim 10^{-11}$ eV, including axion-like particles [1–6], dilatons and moduli [7–9] and fuzzy dark matter [10–12], have been proposed as a potential solution to various problems ranging from fundamental physics to cosmology [1, 3–5, 11, 13–15]. Efforts are underway to search for these ultralight bosons using table-top experiments or astronomical observations [16–31]. When the Compton wavelength of the hypothetical boson is comparable to the size of a black hole (BH) (i.e. $GM\mu_s/\hbar c \sim 1$, where M is the BH mass and μ_s is the boson mass), then a classical wave amplification process (superradiance) forms a bosonic cloud [14, 32–34]. The formation of this cloud extracts rotational energy from the BH until the BH reaches a critical spin set by the Compton frequency of the boson and the mass of BH [14, 34–36]. BHs with spins above the critical spin values will spin down rapidly. The net result of this superradiance process is to create regions where BHs are unlikely to be observed for some particular values of their masses and spins. The exact position and extent of the “exclusion region” depends on the boson mass (e.g. Fig. 2 in Ref. [37]). Given a population of black holes for which masses and spins have been measured, these features in the mass-spin plane can be used to search for ultralight bosons [e.g. 14, 31, 34, 36–49]. Gravitational waves (GWs) are a prime way of accessing this information.

The morphology of GW signals emitted by binary black holes (BBHs) encodes the properties of their sources, including the spins of the two BHs. While the spin measurement of

BHs in X-ray binaries is also possible, it requires modeling of the accretion disk [50–52], which can introduce systematic errors [53]. By contrast, GWs provide a clean and direct measurement of BH spins. Furthermore, measurements made with ground-based GW detectors are complementary since they probe heavier BHs than those usually found in X-ray binaries [54], hence testing the existence of lighter bosons.

However, the measurements of individual BH spins with ground-based detectors such as LIGO and Virgo are usually inconclusive [55–58], making it difficult to set stringent constraints on the boson masses with *individual* sources. Furthermore, the inconclusive spin measurements of individual sources are heavily affected by the prior distribution of black-hole spins at the time of merger, which also depends on the distribution of spins at birth [59–61].

In this paper, therefore, we perform hierarchical Bayesian inference on a *population* of BBHs, to simultaneously infer the mass of the boson and the spin distribution at *formation* [62–70]. We show that the existence of ultralight bosons in the mass range between 10^{-13} eV and 3×10^{-12} eV can be ruled out with $\mathcal{O}(100)$ high signal-to-noise ratio (SNR) BBH detections¹. On the other hand, we illustrate how our method can confirm the existence of bosons in this mass range with two examples of boson masses $\mu_s = 10^{-12}$ eV and 10^{-13} eV, if such bosons exist. Finally, we apply our method to perform the first rigorous spin-based search for ultralight bosons with LIGO and Virgo detections from the first two observing runs [54]. We find no clear statistical evidence to support or reject the existence of ultralight bosons in current data.

* kenkyng@mit.edu

† o.hannuksela@nikhef.nl

¹ In the paper, we define “high SNR” as $\text{SNR} \geq 30$.

II. CRITICAL SPIN ARISING FROM SUPERRADIANT INSTABILITY

GW measurements yield the masses and spins of black holes at merger. Therefore, one needs to account for the impact of superradiance on the evolution of spins, which we quickly review here. Superradiance causes the growth of boson clouds, which spin down their host black hole to characteristic critical spins $\chi_{[nlm]}$ [14, 34, 39] with characteristic growth timescales $\tau_{[nlm]}^{\text{grow}}$. The indices $[nlm]$ are the analog of the hydrogen atom quantum numbers, i.e. a set of radial, orbital azimuthal and magnetic quantum numbers. We follow Dolan's notation, in which the ordinary principal quantum number $\tilde{n} = n + l + m$, such that $n = 0$ corresponds to the dominant (nodeless) modes [71]. One can estimate the BH spin at merger χ_M to be the critical spin of the highest mode $\chi_{[nlm]}$ that is populated in less time than the merger timescale τ_s , i.e. $\tau_{[nlm]}^{\text{grow}} < \tau_s < \tau_{[n(l+1)(m+1)]}^{\text{grow}}$. Explicitly, after the formation of the initial cloud (with timescale $\tau_{[011]}^{\text{grow}}$), the cloud dissipates away emitting nearly monochromatic gravitational waves and leaving a black hole with spin $\chi_{[011]}$. Next, a second and “higher mode” cloud is formed with timescale $\tau_{[022]}^{\text{grow}}$, and the black hole spins down further to the critical spin of this next mode $\chi_{[022]}$, if $\chi_{[011]} > \chi_{[022]}$. This cycle repeats until the black holes merge at time τ_s . In Fig. 1, we show a schematic picture of a system for which both the $l = 1$ and the $l = 2$ clouds have time to form before merger. The growth time of the cloud can be determined theoretically [14, 34, 35, 37, 40]. Refs [34, 35] found that the approximate timescale to form a cloud large enough to spin down the host BH is

$$\tau_{[nlm]}^{\text{grow}} = \tau_{[nlm]}^{\text{inst}}(\mu_s, M, \chi_{I[nlm]}) \log(10^{-4} M / \mu_s), \quad (1)$$

where $\chi_{I[nlm]}$ is the dimensionless spin of the black hole at the onset of superradiance of the $[nlm]$ mode, and $\tau_{[nlm]}^{\text{inst}}$ is the inverse of the superradiant rate $\Gamma_{[nlm]}^{\text{inst}}$, which can be analytically calculated in the long wavelength limit as: [34–36, 72]

$$\begin{aligned} \Gamma_{[nlm]}^{\text{inst}} = & \mu_s (\mu_s M)^{4l+4} (m\chi - 2\mu_s r_+)^{-1} \\ & \times \frac{2^{4l+2} (2l+1+n)!}{(l+1+n)^{2l+4} n!} \left[\frac{l!}{(2l)!(2l+1)!} \right]^2 \\ & \times \prod_{k=1}^l [k^2(1-\chi^2) + (m\chi - 2\mu_s r_+)^2], \end{aligned} \quad (2)$$

where χ is the dimensionless spin of the BH in any instance, $r_+ \equiv M(1 + \sqrt{1 - \chi^2})$ is the radial coordinate of the outer horizon. Typically more massive black holes and lighter bosons will have longer instability timescales, and vice-versa. The instability timescale has also a mild inverse dependence on the dimensionless spin. For a given M and μ_s , a feasible superradiance process requires $\Gamma_{[nlm]}^{\text{inst}}(\mu_s, M, \chi_{I[nlm]}) > 0$. As the superradiant mode grows, the spin angular momentum of the BH is extracted by the cloud, and the instability rate drops until $\Gamma_{[nlm]}^{\text{inst}} = 0$ at saturation.

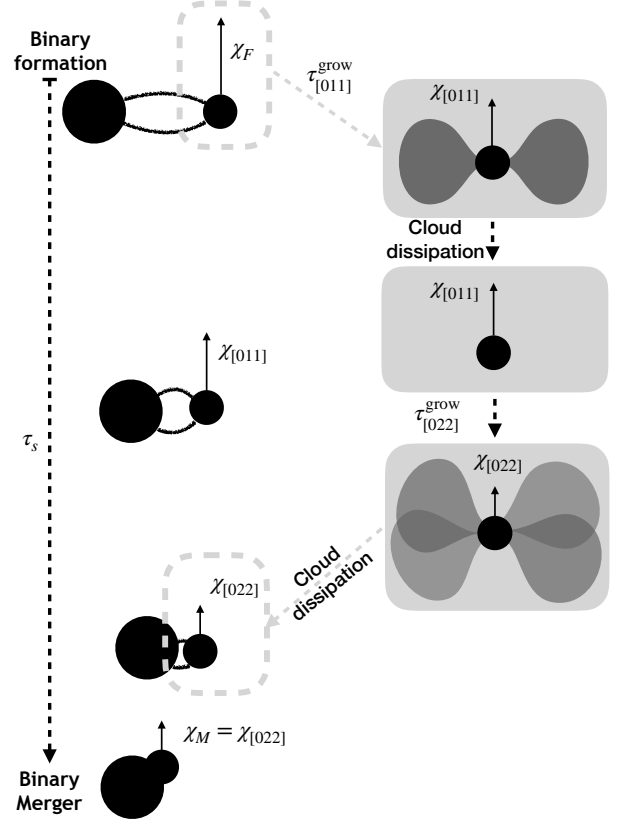


FIG. 1. The possible evolution of a BBH system from formation to merger. The cartoon follows the growth and dissipation of axion clouds around one of the black holes. The black hole starts with a spin a formation χ_F large enough to trigger superradiance. The $n = 0, l = m = 1$ cloud forms with a characteristic timescale $\tau_{[011]}^{\text{grow}}$, lowering the BH spin to $\chi_{[011]}$. The cloud is quickly dissipated through monochromatic GW emission. In this example, the spin of black hole is large enough that a second cloud ($n = 0, l = m = 2$) is also created, which further reduces the black hole spin to $\chi_{[022]}$. At this point the spin of the black hole is too small to trigger the formation of higher-order clouds, and the black hole will merge with spin $\chi_M = \chi_{[022]}$. How many (if any) cloud levels can be populated depends on χ_F and on the timescale for merger τ_s . (The plot is not to scale.)

Besides the spin angular momentum of the BH, a small fraction ($\lesssim 10\%$) of BH mass is also extracted and contributes to the cloud's energy [41]. This is smaller or at most comparable to the mass uncertainty from GW measurements [57]. Therefore, we neglect BH mass loss due to superradiance and assume that the BH masses at merger are the same as the masses at formation.

Note that, in principle, the merger could cause the cloud to fall back to its host through level mixing [34, 47, 73–75]. While one could think that this results in a transfer of the cloud's angular momentum back to the host black hole, which would be spun-up, most in-falling modes have non-positive angular momentum (i.e. $m \leq 0$) due to selection rules. [34, 47, 74, 75]. This is why recent studies have sug-

gested that the in-falling cloud instead *spins down* the host black hole and might decrease the orbital angular momentum [47, 73–77]. An eventual decrease in the BH spin by the fallback would further increase the size of the forbidden region on the mass-spin plane, making it easier to verify the existence of bosons with our method.

We do not allow for boson self-interaction, which would lead to additional phenomenology [34, 37]. We refer to Ref. [31] for the analysis on self-interacting boson using spin measurements of X-ray binaries.

III. TESTING THE ULTRALIGHT-BOSON HYPOTHESIS USING HIERARCHICAL BAYESIAN INFERENCE

An astrophysical distribution of spins at birth, which produces mainly small spins in the absence of superradiance, is partially degenerate with one that produces moderate (or high) spins, in the presence of superradiance². Hence, we need to *simultaneously* infer the spin distribution at birth and the boson mass to properly account for this degeneracy.

We use hierarchical Bayesian inference [65, 67, 68], and consider two competing models: a) in the “boson model”, \mathcal{H}_B , we assume that bosons exist such that BHs can spin down to the corresponding critical spins $\chi_{[nlm]}$ through superradiance (Sec. II); b) in the “astrophysical model”, \mathcal{H}_A , ultralight bosons do not exist, and the spin of BHs merging in binaries is entirely determined by their astrophysical evolution.

The two hypotheses are distinguishable through the resulting distribution of the BH spins at merger. Specifically, for \mathcal{H}_B we assume:

$$\mathcal{H}_B : \chi_M = \begin{cases} \chi_{[nlm]}, & \text{if } \tau_{[nlm]}^{\text{grow}} < \tau_s < \tau_{[n(l+1)(m+1)]}^{\text{grow}} \\ \chi_F, & \text{otherwise} \end{cases} \quad (3)$$

where χ_F and χ_M are the values of the individual BH spins at formation and at merger, respectively, and τ_s is the timescale for the two BHs in the binary to merge. The fact that superradiance only has a finite time to happen, set by the merger timescale τ_s , can be used to estimate their critical spins, based on the instability timescales of the first few dominant modes [14, 34, 37, 40]. In practice, we truncate the superradiance process and extract $\chi_{[nlm]}$ when the instability timescale increases to the BH lifetime before merger, i.e. $\tau_{[nlm]}^{\text{inst}}(\mu_s, M, \chi_{[nlm]}) = \tau_s$. This criterion accounts for the

inefficient superradiance for BHs with $M_i \mu_s \ll 1$. The condition $\tau_{[nlm]}^{\text{grow}} < \tau_s < \tau_{[n(l+1)(m+1)]}^{\text{grow}}$ ensures that $\chi_{[nlm]}$ is obtained at the highest mode within the inspiral time. The growth timescale $\tau_{[nlm]}^{\text{grow}}$ depends on the initial spin, so as $\chi_{[nlm]}$. Therefore, the final value of $\chi_{[nlm]}$ depends on four parameters $(\mu_s, M, \tau_s, \chi_F)$. If, for any $[nlm]$, either χ_F is too small or $M_i \mu_s \gg 1$ such that superradiance is not feasible ($\tau_{[nlm]}^{\text{grow}} < 0$), or the inspiral timescale is shorter than the instability timescale ($\tau_s < \tau_{[nlm]}^{\text{grow}}$), then the merger spin is the same as the formation spin, i.e. $\chi_M = \chi_F$.

On the other hand, there is no superradiance and therefore no spin evolution for \mathcal{H}_A . Thus, the spin remains unchanged from the time of formation to the time of merger:

$$\mathcal{H}_A : \chi_M = \chi_F. \quad (4)$$

For both models, we parameterize the distribution of BH spins at formation with a beta distribution, controlled by two unknown shape parameters $\alpha > 0$ and $\beta > 0$: $p(\chi_F|\alpha, \beta) \propto \chi_F^{\alpha-1} (1 - \chi_F)^{\beta-1}$. This is a generic functional form that can capture multiple different formation pathways [66, 78]. The boson model thus depends on three hyper-parameters $\Lambda_{\mathcal{H}_B} = (\alpha, \beta, \mu_s)$, while the astrophysical model only has two hyper-parameters $\Lambda_{\mathcal{H}_A} = (\alpha, \beta)$. We aim at measuring the hyper-parameters Λ , given a set of N GW observations $\mathbf{d} = \{d_k\}$, whose morphology depends on a set of unknown parameters θ , such as BH masses, spins and distance [79]. The distribution of measured Λ , known as hyper-posterior, can be written as [64, 65, 67–69]:

$$p(\Lambda|\mathbf{d}) \propto \pi(\Lambda) \prod_k^N \left[\frac{1}{\alpha(\Lambda)} \int p(\theta|\Lambda) p(d_k|\theta) d\theta \right] \quad (5)$$

where $p(\theta|\Lambda)$ is the expected distribution of the individual events parameters, given the hyper-population parameters; $\pi(\Lambda)$ are the priors of the hyper-parameters; $p(d_k|\theta)$ is the likelihood of the k -th GW source; and $\alpha(\Lambda)$ is the normalization factor given by

$$\alpha(\Lambda) = \int p(\theta|\Lambda) p_{\text{det}}(\theta) d\theta,$$

where $p_{\text{det}}(\theta)$ is the detection probability for a BBH with parameters θ . The normalization factor $\alpha(\Lambda)$ can be interpreted as the fraction of detectable BBHs.

When working with the boson model, $\Lambda_{\mathcal{H}_B} = (\alpha, \beta, \mu_s)$ and $\theta_{\mathcal{H}_B} = (M_1, M_2, \chi_{M,1}, \chi_{M,2}, \tau_s)$, where M_i and $\chi_{M,i}$ are the masses and spins (at merger) of the two compact objects in the binary. One thus has:

$$p(\Lambda_{\mathcal{H}_B}|\mathbf{d}, \mathcal{H}_B) \propto \pi(\Lambda_{\mathcal{H}_B}) \prod_k^N \left\{ \frac{1}{\alpha(\Lambda_{\mathcal{H}_B})} \int p(d_k|\theta_{\mathcal{H}_B}) \pi(M_1, M_2, \tau_s) \prod_{i=1}^2 [p(\chi_{M,i}|\Lambda_{\mathcal{H}_B}, M_i, \tau_s) dM_i d\chi_{M,i}] d\tau_s \right\}, \quad (6)$$

² Although in the latter case one would expect a characteristic peak at around the critical spin.

In this expression, $\pi(M_1, M_2, \tau_s)$ is the prior on the component masses and the merger time of BBHs, $\pi(\Lambda_{\mathcal{H}_B})$ is the prior on the hyper-parameters of the model \mathcal{H}_B , and $p(\chi_{M,i}|\Lambda_{\mathcal{H}_B}, M_i, \tau_s)$ is the distribution of the spin-magnitude at merger of \mathcal{H}_B . This latter can be derived from the spin-magnitude distribution at formation as:

$$\begin{aligned} p(\chi_{M,i}|\alpha, \beta, \mu_s, M_i, \tau_s) \\ = \int_0^1 p(\chi_{M,i}|\mu_s, M_i, \tau_s, \chi_{F,i}) p(\chi_{F,i}|\alpha, \beta) d\chi_{F,i}, \end{aligned} \quad (7)$$

in which we define the conditional probability:

$$\begin{aligned} p(\chi_{M,i}|\mu_s, M_i, \tau_s, \chi_{F,i}) \\ = \delta[\chi_{M,i} - \chi_{[nlm]}(\mu_s, M_i, \tau_s, \chi_{F,i})] \Theta[\chi_{F,i} - \chi_{[nlm]}] \\ + \delta(\chi_{M,i} - \chi_{F,i}) \Theta[\chi_{[nlm]} - \chi_{F,i}], \end{aligned} \quad (8)$$

where $\delta[\dots]$ is the Dirac-delta function that maps from the spin at formation to the spin at merger and $\Theta[\dots]$ is the Heaviside step function that enforces the superradiance condition $\chi_{F,i} > \chi_{[nlm]}$. As the growth timescale $\tau_{[nlm]}^{\text{grow}}$ depends on the initial spin at the superradiance onset, one needs to calculate $\chi_{[nlm]}$ for each $\chi_{F,i}$ to precisely calculate the integral in Eq. (7). To facilitate the evaluation of this integral during the sampling process, we mitigate the dependence of $\chi_{F,i}$ in $\chi_{[nlm]}$ by the following approximations to fix the values of $\chi_{I[nlm]}$. For the dominant [011] mode, we set the spin at the onset to the midpoint between the minimum spin value required for superradiance to happen and the maximal Kerr spin: $\chi_{I[011]} \approx (1 + \chi_{[011]})/2$. This is justified because the growth timescale varies by only around one order of magnitude for spins in the range $\chi_{I[011]} \in [\chi_{[011]}, 1]$. After spin-down, the black hole settles on the critical spin of the given mode, $\chi_{[nlm]}$. Therefore, we approximate the initial spin of each subsequent mode $\chi_{[n(l+1)(m+1)]}$ by the preceding mode critical spin, i.e. $\chi_{I[n(l+1)(m+1)]} \approx \chi_{[nlm]}$. With the above simplifications, the values of $\chi_{[nlm]}$ only depend on (μ_s, M_i, τ_s) and we can approximate Eq. (7) as

$$\begin{aligned} p(\chi_{M,i}|\alpha, \beta, \mu_s, M_i, \tau_s) \approx f_{\text{SR}} \delta(\chi_{M,i} - \chi_{[nlm]}) \\ + p(\chi_{M,i}|\alpha, \beta) \Theta(\chi_{[nlm]} - \chi_{M,i}), \end{aligned} \quad (9)$$

with f_{SR} is the *differential* fraction of BHs that undergo superradiance at BH mass M_i :

$$\begin{aligned} f_{\text{SR}}(\mu_s, M_i, \tau_s, \alpha, \beta) \\ \equiv \int_0^1 p(\chi_{F,i}|\alpha, \beta) \Theta[\chi_{F,i} - \chi_{[nlm]}(\mu_s, M_i, \tau_s)] d\chi_{F,i}. \end{aligned} \quad (10)$$

In the astrophysical model, \mathcal{H}_A , one obtains a similar expression for $p(\Lambda_{\mathcal{H}_A}|\mathbf{d}, \mathcal{H}_A)$ by replacing $\mathcal{H}_B \rightarrow \mathcal{H}_A$ everywhere, and removing all references to τ_s , which is not a relevant parameter of \mathcal{H}_A .

While calculating Eq. (6), we use a power law prior $\pi(M_1) \propto M_1^{-2.35}$ for the primary mass [80], and uniform

prior for mass ratio $q = M_2/M_1$ with $M_2 \leq M_1$. We also assume that τ_s is known (for the \mathcal{H}_B model) and fixed at 10 Myr: $\pi(\tau_s) = \delta(\tau_s - 10 \text{ Myr})$, which is toward the lower limit of typical merger times, according to numerical simulations ($\sim 10 \text{ Myr} - \sim 10 \text{ Gyr}$) [81–91]. From one side, this choice is conservative as it allows for the least time for BHs to spin-down due to superradiance, making it harder to find evidence for bosons. From the other, restricting the merger time prior overestimates the prior information thus overestimates the evidence for the boson hypothesis \mathcal{H}_B in Eq. (6). Nevertheless, the additional parameter space in τ_s is expected to contribute modestly to the Bayes factor because the corrections to the available mass-spin parameter space are mostly smaller than the mass-spin measurement uncertainties. Therefore, while more realistic models for the merger time prior $\pi(\tau_s)$ could be used, our choice is sufficient for advanced detectors, given their limited precision in the measurement of component masses and spins.

Since we assume the BH mass distribution is known, we do not need to consider its selection effect while calculating α . We can also ignore selection effects due to BH spins as the expected number of observations only varies by $\lesssim 10\%$ for different spin models [62, 78, 92]. Furthermore, for Λ_B , the fraction of detectable BBHs does not depend on μ_s . Based on the above arguments, we therefore assume $\alpha(\Lambda_{\mathcal{H}_B})$ and $\alpha(\Lambda_{\mathcal{H}_A})$ are constants in the evaluation of the hyper-posteriors. In generating the simulations, however, we fully account for all selection effects so that the number of sources can be interpreted as the expected number of detections in future observations.

Integrating Eq. (6), and the equivalent expression for \mathcal{H}_A , over the whole hyper-parameters space yields evidences $Z_{\mathcal{H}_B}$ and $Z_{\mathcal{H}_A}$ that can be used to calculate Bayes factor between the boson and astrophysical hypothesis: $\mathcal{B}_A^B = Z_{\mathcal{H}_B}/Z_{\mathcal{H}_A}$. We also perform a Monte Carlo simulation of 50 different sets of sources in every simulated Universe. This allows us to estimate the probability distribution of Bayes factor due to Poisson fluctuation for every values of N .

IV. MOCK DATA ANALYSIS AND O1/O2 SEARCH

The method described above can be applied to both simulated and real detections. We first demonstrate its use on three different simulated “universes”: (i) one with a boson scalar field with $\mu_s = 10^{-13} \text{ eV}$; (ii) one with a boson scalar field with $\mu_s = 10^{-12} \text{ eV}$ and (iii) one where no boson exists (“astrophysical population”). To create the mock populations, we generate BBHs with component masses $M_{1,2}$ following the same prior in the model: $\pi(M_1) \propto M_1^{-2.35}$, uniform distribution for q in $[0.1, 1]$ and require both $\{M_1, M_2\} \in [5, 50] M_\odot$, consistently with Ref [66]. The BBHs are distributed uniformly in source-frame comoving volume, sky positions, orbital orientations and polarization angles in the unit-sphere. The astrophysical processes that set the initial spin magnitude and orientation are still to be fully understood [59–61, 93]. For each of the three universes, we consider two distributions of *formation* spin magnitudes $\chi_{F,i}$: (a) uniform in $[0, 1]$ (“flat spin”) and (b) $p(\chi_{F,i}) \propto (1 - \chi_{F,i})$ (“low spin”), with an

isotropic spin orientation in both cases. The shape parameters of beta distribution are $\alpha = \beta = 1$ for “flat spin” and $\alpha = 1, \beta = 2$ for “low spin”.

When simulating the universes where bosons exist, we need to convert the BH spins at formation to the spins at merger using Eq. (3). We assume all BBHs have a short merger timescale $\tau_s = 10$ Myr, which minimizes the effect of superradiance and is thus a conservative choice. To maintain the computational cost of the analysis reasonable, of all the sources we generate, we only analyze those for which $\text{SNR} > 30$. These are the only sources that will contribute to the test since individual spins are hard to measure for low or medium SNR BBHs [55, 57]. The populations of synthetic BBH sources are thus added into simulated noise of the LIGO and Virgo detectors at design sensitivity [94, 95]. We use the LALINFERENCE [96, 97] algorithm with the IMRPHENOMPv2 waveform family [98] to obtain posterior and likelihood distributions for the compact binary parameters of the simulated sources, which can be used to infer the population hyper-parameters as described in the previous section. For all of the hyper-parameters, we use uniform-in-log priors, with ranges $[0.01, 10]$ for α and β , as well as $[10^{-13}, 3 \times 10^{-12}]$ eV for μ_s , which is the range of μ_s that can be realistically probed with ground-based GW detectors [39].

In Fig. 2, we show the evolution of the log Bayes factor boson vs. astrophysical model, $\log_{10} \mathcal{B}_A^B$ as more events are used for the test. The bottom x -axis show the number of loud events, while the top one shows the number of total events ³.

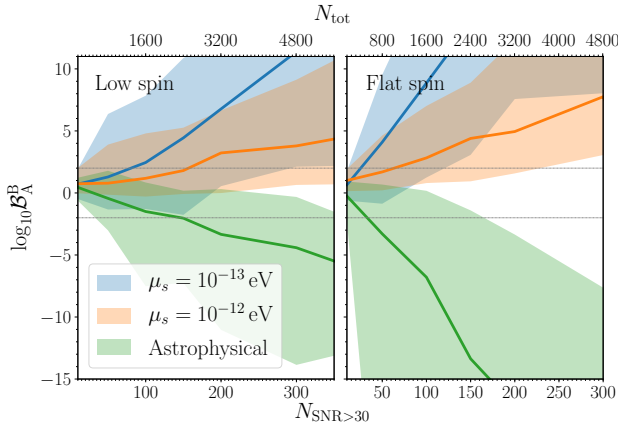


FIG. 2. The \log_{10} Bayes factor between the boson and astrophysical hypothesis as a function of the number of sources $N_{\text{SNR}>30}$ from the boson with $\mu_s = 10^{-13}$ eV (blue), boson with $\mu_s = 10^{-12}$ eV (orange) and astrophysical (green) populations. For each population, we repeat the analysis with the “low spin” (left panel) and “flat spin” (right panel) distribution at formation. The solid lines and colored bands are medians and 90% credible intervals over 50 realizations of a population with $N_{\text{SNR}>30}$ sources. The two horizontal lines show $\mathcal{B}_A^B = 0.01$ and 100.

³ Since the distribution of SNRs for BBH detected by advanced detectors is known analytically and goes as $P(\rho) \propto \rho^{-4}$ [99], one can calculate that there is one event with $\text{SNR} > 30$ for each 16 events with $\text{SNR} \geq 12$ on average.

TABLE I. The estimated numbers of high SNR detections to rule out (confirm) bosons for different combinations of formation spin distribution and boson.

Population models	Flat spin	Low spin
Astrophysical ^a	30^{+135}_{-25}	140^{+120}_{-105}
$\mu_s = 10^{-13}$ eV ^b	25^{+95}_{-15}	80^{+210}_{-70}
$\mu_s = 10^{-12}$ eV ^b	65^{+165}_{-55}	155^{+345}_{-145} ^c

^a The statistical requirement is $\mathcal{B}_A^B = 0.01$ to rule out bosons within $[10^{-13}, 3 \times 10^{-12}]$ eV.

^b The statistical requirement is $\mathcal{B}_A^B = 100$ to confirm the bosons.

^c The upper bound is only an approximation since all simulated GWs are exhausted before reaching the desired $\mathcal{B}_A^B = 100$.

All curves show that the method correctly prefers the correct model, given enough number of observations. In Table I, we report the expected numbers of observations required to significantly ⁴ prefer a hypothesis for all the spin distribution and boson mass pairs. In general, we would expect that fewer sources are required to disprove the boson hypothesis than to confirm it. This is because even one highly spinning BH measurement can contradict \mathcal{H}_B , whereas multiple BHs that match the predicted critical spins are necessary to favor \mathcal{H}_B . On the other hand, disfavoring the astrophysical model can also happen quickly if the boson mass and the formation spins are such that the spin distribution at the merging time cannot possibly be captured with a beta distribution, which decreases the likelihood. This is why we predict smaller numbers on average to confirm $\mu_s = 10^{-13}$ eV than to rule out the boson mass range between 10^{-13} eV $\leq \mu_s \leq 3 \times 10^{-12}$ eV in both “flat spin” and “low spin” scenarios. We also notice that more sources are required for the test if BHs generally have low formation spins (“low spin” population) than for the “flat spin” population. This is expected since it is harder to prove the existence of a dearth of highly spinning BHs given a population with small formation spins.

Next, we look at the estimation of the individual hyper-parameters. As an example, we take 300 high SNR detections drawn from the simulated Universe with “flat spin” and $\mu_s = 10^{-12}$ eV. Figure 3 shows the corner plot of (α, β, μ_s) in \log_{10} space, assuming \mathcal{H}_B (blue) or \mathcal{H}_A (orange). First, we notice the model \mathcal{H}_B obtains a bimodal hyper-posterior for μ_s . This is due to the higher-modes in superradiance for the same BH mass but larger μ_s . We note that the true μ_s is found at the primary peak, and the secondary peak becomes less prominent as the number of detections increases. Second, using the astrophysical model \mathcal{H}_A , we recover heavily biased values of (α, β) , which control the shape of the spins at formation. To better visualize this bias, we recast the (α, β) hyper-posteriors of both models into $p(\chi_F|\alpha, \beta)$, as shown in Fig. 4. The model \mathcal{H}_A (orange band) is indeed more consistent with the spin distribution at merger $p(\chi_M|\alpha = 1, \beta = 1, \mu_s = 10^{-12}$ eV) (black dashed line), instead of the distribution at formation $p(\chi_F|\alpha = 1, \beta = 1)$ (black solid line). This

⁴ We follow Ref. [100] and strongly prefer the boson (astrophysical) hypothesis if $\mathcal{B}_A^B \geq 100$ (≤ 0.01).

is not surprising, since \mathcal{H}_A cannot account for the superradiant spin-loss and it mistakes the apparently low-spin distribution $p(\chi_M)$ for $p(\chi_F)$. On the other hand, \mathcal{H}_B (blue band) can “undo” the superradiance and reconstruct $p(\chi_F)$ much closer to the “true” distribution at formation (black solid line) in our simulation. Hence, both the hyper-posterior and the χ_F distribution, inferred by the model \mathcal{H}_B , are unbiased.

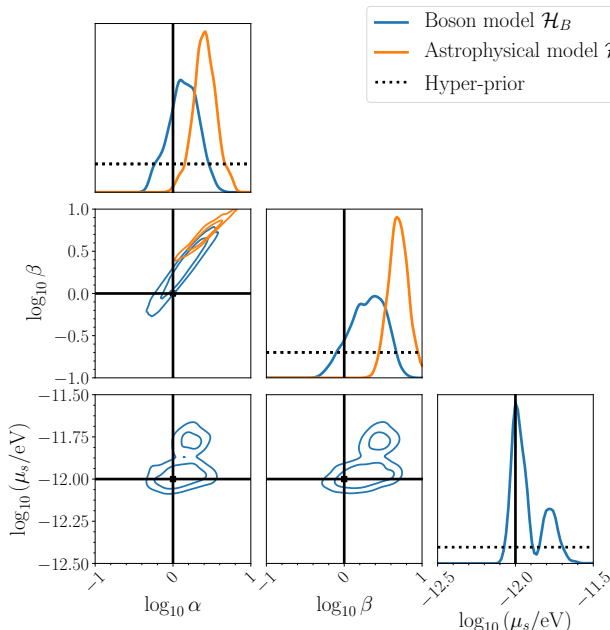


FIG. 3. Corner plots of the (α, β, μ_s) hyper-posterior assuming boson model \mathcal{H}_B (blue) and \mathcal{H}_A (orange) in \log_{10} space. The contours are shown at 68% and 95% intervals. For this example, we average 50 sets of sources, each with 300 high SNR events drawing from the boson population at $\mu_s = 10^{-12}$ eV and $(\alpha, \beta) = (1, 1)$ (“flat spin”). The dashed and solid black lines are the hyper-priors and “true” values, respectively.

Finally, we apply our method to the 10 BBHs released by the LIGO and Virgo collaborations [54, 101, 102]. We follow the same methodologies for the hierarchical inference as in Sec. III, assuming the boson mass to be flat in log in the range 10^{-13} eV $\leq \mu_s \leq 3 \times 10^{-12}$ eV, as expected of the ultralight bosons probed by the binary black holes in the LIGO/Virgo range ($\sim 5 - \sim 50 M_\odot$ [54, 101, 102]). We find a Bayes factor of ~ 2.4 in favor of the boson hypothesis. Therefore, the current data do not allow drawing any statistically significant conclusions

V. DISCUSSION

In this paper, we have shown that BBHs detected by ground-based GW detectors can be used to rule out the existence of ultralight bosons in the mass range $[10^{-13}, 3 \times 10^{-12}]$ eV. Our method is also capable to reveal their existence, as we have shown with two example masses $\mu_s = 10^{-13}$ eV and 10^{-12} eV. We have generated populations of

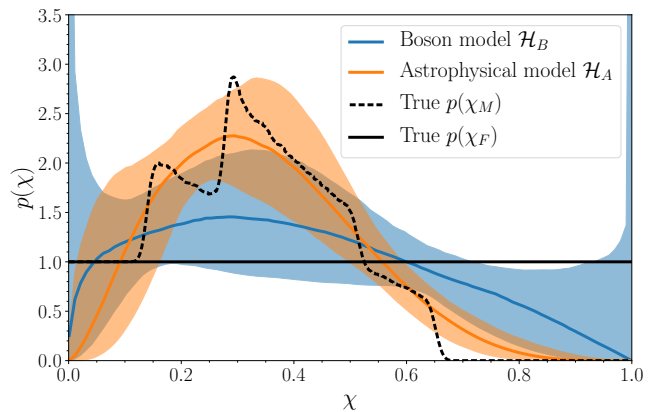


FIG. 4. Hyper-posterior of the spin distribution at formation $p(\chi_F|\alpha, \beta)$, inferred with the same set of simulations (“flat” spin and $\mu_s = 10^{-12}$ eV) in Fig. 3. The blue (orange) solid line shows the median of the inferred $p(\chi_F|\alpha, \beta)$ assuming \mathcal{H}_B (\mathcal{H}_A). The bands mark the 90% credible intervals. The dashed and solid black lines are the “true” spin distribution at merger and at formation, respectively, in this simulation with boson existence. The characteristic “zig-zag” structure in $p(\chi_M)$ reflects the critical spins of different superradiant modes.

simulated BBHs with a uniform distribution and a linearly-decreasing distribution of spins at formation to investigate the impact of spin distribution at formation on the statistical power of our proposed method. The morphology of the “exclusion regions” in the BH mass-spin plane generated by bosons in the mass range of $[10^{-12}, 10^{-13}]$ eV varies smoothly with the boson mass [39]. Therefore, we conclude that combining $\lesssim 300$ high-SNR events may be enough to rule out or confirm the existence of an ultralight boson within the full range $[10^{-13}, 10^{-12}]$ eV.

Applying the same method to the 10 BBH published by LIGO and Virgo yields inconclusive results. This is not surprising based on the results of our simulations. While we only consider scalar field bosons in this study, the method we developed is applicable to vector or tensor boson fields, which have much shorter instability and GW emission timescales [6, 103, 104]. Our analysis of simulated BBHs has made a few simplifying assumptions which make it conservative. First, we have assumed that all BBH merge in 10 Myr, which is toward the lower limit of what is usually obtained in numerical simulations [81–91]. Since most of the BBHs in our parameters space of interest would have undergone superradiance within 10 Myr except for the very low mass systems $\sim 5M_\odot - 5M_\odot$, assuming longer merger times does not significantly improve the searching efficiency. Second, we have assumed that only sources with $\text{SNR} > 30$ will contribute to this test, as their spins are easier to measure. In reality, while the component spins of weaker events are harder to measure, they will still contribute for the test. The true distribution of spins at formation plays the most important role: the number of events needed to perform this test will be larger if the astrophysical distribution of spins at formation is such that small spins are preferred. Conversely, if many

highly-spinning BHs are formed, potentially with significant misalignment between spin and angular momentum (both of which makes spins easier to measure), then fewer sources will be necessary. Given the measured BBH merger rate, ground-based interferometers will detect hundreds of BBHs per year at design sensitivity [105–109]. In the analysis, we ignored the $\lesssim 10\%$ mass loss during superradiance. In order to assess the impact of this choice, we repeated the analysis with the BH mass posteriors shifted by 5% toward the light side, hence mimicking the effect of mass loss. This translates to a systematic overestimation of $\sim 5\%$ boson mass in linear scale, which is still within the statistical uncertainty, in our inference with $\mathcal{O}(100)$ high SNR sources. However, we expect this systematic error will dominate when the number of events grow to $\mathcal{O}(10^4)$ in the era of next-generation detectors [110–117]. In this large-number observations regime, one will want to use more sophisticated models which also capture eventual correlations between the masses and spin of astrophysical BHs [59, 60, 93]. This may boost or reduce the statistical power of testing boson hypothesis in different boson mass range, depending on the actual joint distribution of BH mass and spin at formation. We will leave investigating these systematics to future work. Within the assumptions made in this study, it seems feasible to rule out the existence of ultralight bosons with a few years of advanced detectors data. Statistically proving the existence of these bosons will take longer, as more sources are required: the planned upgrades of LIGO and Virgo to their “plus” configurations might yield thousands of BBH events per year, which will make it

more plausible to gather evidence for the existence of ultralight bosons [111, 113].

VI. ACKNOWLEDGEMENTS

We thank Emanuele Berti, Richard Brito, Will Farr, Carl Haster, Max Isi and Kaze Wong for valuable discussions and suggestions. KKYN and SV acknowledge the support of the National Science Foundation, the LIGO Laboratory and the LIGO Data Grid clusters. LIGO was constructed by the California Institute of Technology and Massachusetts Institute of Technology with funding from the National Science Foundation and operates under cooperative agreement PHY-1764464. OAH was supported by the Hong Kong Ph.D. Fellowship Scheme (HKPFS) issued by the Research Grants Council (RGC) of Hong Kong before resubmission and is supported by the research program of the Netherlands Organization for Scientific Research (NWO). TGFL was partially supported by grants from the Research Grants Council of Hong Kong (Project No. CUHK14306218, CUHK14310816 and CUHK24304317), Research Committee of the Chinese University of Hong Kong and the Croucher Foundation in Hong Kong. This research has made use of data, software and/or web tools obtained from the Gravitational Wave Open Science Center (<https://www.gw-openscience.org>), a service of LIGO Laboratory, the LIGO Scientific Collaboration and the Virgo Collaboration.

-
- [1] R. D. Peccei and H. R. Quinn, CP conservation in the presence of pseudoparticles, *Phys. Rev. Lett.* **38**, 1440 (1977).
 - [2] R. D. Peccei and H. R. Quinn, Constraints imposed by CP conservation in the presence of pseudoparticles, *Phys. Rev. D* **16**, 1791 (1977).
 - [3] S. Weinberg, A new light boson?, *Phys. Rev. Lett.* **40**, 223 (1978).
 - [4] F. Wilczek, Problem of strong p and t invariance in the presence of instantons, *Phys. Rev. Lett.* **40**, 279 (1978).
 - [5] R. D. Peccei, The strong cp problem and axions, in *Axions* (Springer, 2008) pp. 3–17.
 - [6] V. Cardoso, O. J. C. Dias, G. S. Hartnett, M. Middleton, P. Pani, and J. E. Santos, Constraining the mass of dark photons and axion-like particles through black-hole superradiance, *JCAP* **1803** (03), 043, arXiv:1801.01420 [gr-qc].
 - [7] S. Dimopoulos and G. F. Giudice, Macroscopic forces from supersymmetry, *Physics Letters B* **379**, 105 (1996), arXiv:hep-ph/9602350 [hep-ph].
 - [8] T. Damour and J. F. Donoghue, Equivalence principle violations and couplings of a light dilaton, *Phys. Rev. D* **82**, 084033 (2010).
 - [9] A. Arvanitaki, J. Huang, and K. Van Tilburg, Searching for dilaton dark matter with atomic clocks, *Phys. Rev. D* **91**, 015015 (2015), arXiv:1405.2925 [hep-ph].
 - [10] W. Hu, R. Barkana, and A. Gruzinov, Fuzzy cold dark matter: the wave properties of ultralight particles, *Physical Review Letters* **85**, 1158 (2000).
 - [11] L. Hui, J. P. Ostriker, S. Tremaine, and E. Witten, Ultralight scalars as cosmological dark matter, *Phys. Rev. D* **95**, 043541 (2017), arXiv:1610.08297 [astro-ph.CO].
 - [12] H.-Y. Schive, T. Chiueh, and T. Broadhurst, Cosmic Structure as the Quantum Interference of a Coherent Dark Wave, *Nature Phys.* **10**, 496 (2014), arXiv:1406.6586 [astro-ph.GA].
 - [13] G. Bertone, D. Hooper, and J. Silk, Particle dark matter: Evidence, candidates and constraints, *Phys. Rept.* **405**, 279 (2005), arXiv:hep-ph/0404175 [hep-ph].
 - [14] A. Arvanitaki, S. Dimopoulos, S. Dubovsky, N. Kaloper, and J. March-Russell, String Axiverse, *Phys. Rev. D* **81**, 123530 (2010), arXiv:0905.4720 [hep-th].
 - [15] D. J. E. Marsh, Axion Cosmology, *Phys. Rept.* **643**, 1 (2016), arXiv:1510.07633 [astro-ph.CO].
 - [16] A. Wagner *et al.*, Search for hidden sector photons with the admx detector, *Phys. Rev. Lett.* **105**, 171801 (2010).
 - [17] S. J. Asztalos *et al.*, Squid-based microwave cavity search for dark-matter axions, *Phys. Rev. Lett.* **104**, 041301 (2010).
 - [18] G. Rybka *et al.*, Search for chameleon scalar fields with the axion dark matter experiment, *Phys. Rev. Lett.* **105**, 051801 (2010).
 - [19] M. Arik, S. Aune, K. Barth, A. Belov, S. Borghi, H. Bräuninger, G. Cantatore, J. M. Carmona, S. A. Cetin, J. I. Collar, *et al.* (CAST Collaboration), Search for sub-ev mass solar axions by the cern axion solar telescope with ^3He buffer gas, *Phys. Rev. Lett.* **107**, 261302 (2011).
 - [20] P. Pagnat *et al.* (OSQAR), Search for weakly interacting sub-eV particles with the OSQAR laser-based experiment:

- results and perspectives, *Eur. Phys. J. C* **74**, 3027 (2014), arXiv:1306.0443 [hep-ex].
- [21] P. S. Corasaniti, S. Agarwal, D. J. E. Marsh, and S. Das, Constraints on dark matter scenarios from measurements of the galaxy luminosity function at high redshifts, *Phys. Rev. D* **95**, 083512 (2017).
- [22] J. Choi, H. Themann, M. J. Lee, B. R. Ko, and Y. K. Semertzidis, First axion dark matter search with toroidal geometry, *Phys. Rev. D* **96**, 061102 (2017).
- [23] D. S. Akerib, S. Alsum, C. Aquino, H. M. Araújo, X. Bai, A. J. Bailey, J. Balajthy, P. Beltrame, E. P. Bernard, A. Bernstein, T. P. Biesiadzinski, *et al.* (LUX Collaboration), First searches for axions and axionlike particles with the lux experiment, *Phys. Rev. Lett.* **118**, 261301 (2017).
- [24] B. Brubaker *et al.*, First results from a microwave cavity axion search at 24 μeV , *Phys. Rev. Lett.* **118**, 061302 (2017), arXiv:1610.02580 [astro-ph.CO].
- [25] Y. J. Kim, P.-H. Chu, and I. Savukov, Experimental constraint on an exotic spin- and velocity-dependent interaction in the sub-meV range of axion mass with a spin-exchange relaxation-free magnetometer, *Phys. Rev. Lett.* **121**, 091802 (2018).
- [26] A. Garcon *et al.*, The cosmic axion spin precession experiment (CASPER): a dark-matter search with nuclear magnetic resonance, *Quantum Science and Technology* **3**, 014008 (2018), arXiv:1707.05312 [physics.ins-det].
- [27] J. L. Ouellet, C. P. Salemi, J. W. Foster, R. Henning, Z. Bogorad, J. M. Conrad, J. A. Formaggio, Y. Kahn, J. Minervini, A. Radovinsky, N. L. Rodd, B. R. Safdi, J. Thaler, D. Winkler, and L. Winslow, First results from abracadabra-10 cm: A search for sub- μeV axion dark matter, *Phys. Rev. Lett.* **122**, 121802 (2019).
- [28] H. Davoudiasl and P. B. Denton, Ultralight Boson Dark Matter and Event Horizon Telescope Observations of M 87*, *Phys. Rev. Lett.* **123**, 021102 (2019), arXiv:1904.09242 [astro-ph.CO].
- [29] C. Abel *et al.*, Search for Axionlike Dark Matter through Nuclear Spin Precession in Electric and Magnetic Fields, *Phys. Rev. X* **7**, 041034 (2017), arXiv:1708.06367 [hep-ph].
- [30] H. Grote and Y. V. Stadnik, Novel signatures of dark matter in laser-interferometric gravitational-wave detectors, *Phys. Rev. Research* **1**, 033187 (2019), arXiv:1906.06193 [astro-ph.IM].
- [31] N. Fernandez, A. Ghalsasi, and S. Profumo, Superradiance and the Spins of Black Holes from LIGO and X-ray binaries, arXiv e-prints, arXiv:1911.07862 (2019), arXiv:1911.07862 [hep-ph].
- [32] Y. B. Zel'Dovich, Generation of Waves by a Rotating Body, *Soviet Journal of Experimental and Theoretical Physics Letters* **14**, 180 (1971).
- [33] W. H. Press and S. A. Teukolsky, Floating Orbits, Superradiant Scattering and the Black-hole Bomb, *Nature* **238**, 211 (1972).
- [34] A. Arvanitaki and S. Dubovsky, Exploring the String Axiverse with Precision Black Hole Physics, *Phys. Rev. D* **83**, 044026 (2011), arXiv:1004.3558 [hep-th].
- [35] R. Brito, V. Cardoso, and P. Pani, Black holes as particle detectors: evolution of superradiant instabilities, *Class. Quant. Grav.* **32**, 134001 (2015), arXiv:1411.0686 [gr-qc].
- [36] R. Brito, V. Cardoso, and P. Pani, Superradiance, *Lect. Notes Phys.* **906**, pp.1 (2015), arXiv:1501.06570 [gr-qc].
- [37] A. Arvanitaki, M. Baryakhtar, and X. Huang, Discovering the QCD Axion with Black Holes and Gravitational Waves, *Phys. Rev. D* **91**, 084011 (2015), arXiv:1411.2263 [hep-ph].
- [38] A. Arvanitaki, M. Baryakhtar, S. Dimopoulos, S. Dubovsky, and R. Lasenby, Black Hole Mergers and the QCD Axion at Advanced LIGO, *Phys. Rev. D* **95**, 043001 (2017), arXiv:1604.03958 [hep-ph].
- [39] R. Brito, S. Ghosh, E. Barausse, E. Berti, V. Cardoso, I. Dvorkin, A. Klein, and P. Pani, Gravitational wave searches for ultralight bosons with LIGO and LISA, *Phys. Rev. D* **96**, 064050 (2017), arXiv:1706.06311 [gr-qc].
- [40] R. Brito, S. Ghosh, E. Barausse, E. Berti, V. Cardoso, I. Dvorkin, A. Klein, and P. Pani, Stochastic and resolvable gravitational waves from ultralight bosons, *Phys. Rev. Lett.* **119**, 131101 (2017), arXiv:1706.05097 [gr-qc].
- [41] M. Isi, L. Sun, R. Brito, and A. Melatos, Directed searches for gravitational waves from ultralight bosons, *Phys. Rev. D* **99**, 084042 (2019), [Erratum: *Phys. Rev. D* **102**, 049901 (2020)], arXiv:1810.03812 [gr-qc].
- [42] S. D'Antonio *et al.*, Semicoherent analysis method to search for continuous gravitational waves emitted by ultralight boson clouds around spinning black holes, *Phys. Rev. D* **98**, 103017 (2018), arXiv:1809.07202 [gr-qc].
- [43] S. Ghosh, E. Berti, R. Brito, and M. Richartz, Follow-up signals from superradiant instabilities of black hole merger remnants, *Phys. Rev. D* **99**, 104030 (2019), arXiv:1812.01620 [gr-qc].
- [44] L. Tsukada, T. Callister, A. Matas, and P. Meyers, First search for a stochastic gravitational-wave background from ultralight bosons, *Phys. Rev. D* **99**, 103015 (2019), arXiv:1812.09622 [astro-ph.HE].
- [45] M. J. Stott, D. J. E. Marsh, C. Pongkitivanichkul, L. C. Price, and B. S. Acharya, Spectrum of the axion dark sector, *Phys. Rev. D* **96**, 083510 (2017), arXiv:1706.03236 [astro-ph.CO].
- [46] O. A. Hannuksela, K. W. Wong, R. Brito, E. Berti, and T. G. Li, Probing the existence of ultralight bosons with a single gravitational-wave measurement, *Nature Astron.* **3**, 447 (2019), arXiv:1804.09659 [astro-ph.HE].
- [47] E. Berti, R. Brito, C. F. Macedo, G. Raposo, and J. L. Rosa, Ultralight boson cloud depletion in binary systems, *Physical Review D* **99**, 104039 (2019).
- [48] C. Palomba *et al.*, Direct constraints on ultra-light boson mass from searches for continuous gravitational waves, *Phys. Rev. Lett.* **123**, 171101 (2019), arXiv:1909.08854 [astro-ph.HE].
- [49] K. K. Ng, M. Isi, C.-J. Haster, and S. Vitale, Multiband gravitational-wave searches for ultralight bosons, arXiv e-prints (2020), arXiv:2007.12793 [gr-qc].
- [50] A. C. Fabian, M. J. Rees, L. Stella, and N. E. White, X-ray fluorescence from the inner disc in Cygnus X-1., *MNRAS* **238**, 729 (1989).
- [51] C. S. Reynolds and M. A. Nowak, Fluorescent iron lines as a probe of astrophysical black hole systems, *Phys. Rept.* **377**, 389 (2003), arXiv:astro-ph/0212065 [astro-ph].
- [52] J. E. McClintock, R. Narayan, S. W. Davis, L. Gou, A. Kulkarni, J. A. Orosz, R. F. Penna, R. A. Remillard, and J. F. Steiner, Measuring the Spins of Accreting Black Holes, *General relativity and gravitation. Proceedings, 19th International Conference, GR19, Mexico City, Mexico, July 4-9, 2010*, *Class. Quant. Grav.* **28**, 114009 (2011), arXiv:1101.0811 [astro-ph.HE].
- [53] S. N. Zhang, W. Cui, and W. Chen, Black hole spin in X-ray binaries: Observational consequences, *Astrophys. J.* **482**, L155 (1997), arXiv:astro-ph/9704072 [astro-ph].
- [54] B. Abbott *et al.* (LIGO Scientific, Virgo), GWTC-1: A Gravitational-Wave Transient Catalog of Compact Binary Mergers Observed by LIGO and Virgo during the First and Second Observing Runs, *Phys. Rev. X* **9**, 031040 (2019), arXiv:1811.12907 [astro-ph.HE].
- [55] S. Vitale, R. Lynch, J. Veitch, V. Raymond, and R. Sturani, Measuring the Spin of Black Holes in Binary Systems Us-

- ing Gravitational Waves, *Phys. Rev. Lett.* **112**, 251101 (2014), arXiv:1403.0129 [gr-qc].
- [56] M. Pürrer, M. Hannam, and F. Ohme, Can we measure individual black-hole spins from gravitational-wave observations?, *Phys. Rev. D* **93**, 084042 (2016), arXiv:1512.04955 [gr-qc].
- [57] S. Vitale, R. Lynch, V. Raymond, R. Sturani, J. Veitch, and P. Graff, Parameter estimation for heavy binary-black holes with networks of second-generation gravitational-wave detectors, *Phys. Rev. D* **95**, 064053 (2017), arXiv:1611.01122 [gr-qc].
- [58] S. Fairhurst, R. Green, C. Hoy, M. Hannam, and A. Muir, Two-harmonic approximation for gravitational waveforms from precessing binaries, *Phys. Rev. D* **102**, 024055 (2020), arXiv:1908.05707 [gr-qc].
- [59] K. Belczynski *et al.*, Evolutionary roads leading to low effective spins, high black hole masses, and O1/O2 rates for LIGO/Virgo binary black holes, *Astron. Astrophys.* **636**, A104 (2020), arXiv:1706.07053 [astro-ph.HE].
- [60] D. Gerosa, E. Berti, R. O’Shaughnessy, K. Belczynski, M. Kesden, D. Wysocki, and W. Gladysz, Spin orientations of merging black holes formed from the evolution of stellar binaries, *Phys. Rev. D* **98**, 084036 (2018), arXiv:1808.02491 [astro-ph.HE].
- [61] K. A. Postnov and A. G. Kuranov, Black hole spins in coalescing binary black holes, *MNRAS* **483**, 3288 (2019), arXiv:1706.00369 [astro-ph.HE].
- [62] W. M. Farr, S. Stevenson, M. C. Miller, I. Mandel, B. Farr, and A. Vecchio, Distinguishing spin-aligned and isotropic black hole populations with gravitational waves, *Nature* **548**, 426 (2017).
- [63] J. Roulet and M. Zaldarriaga, Constraints on binary black hole populations from LIGO–Virgo detections, *Mon. Not. Roy. Astron. Soc.* **484**, 4216 (2019), arXiv:1806.10610 [astro-ph.HE].
- [64] E. Thrane and C. Talbot, An introduction to Bayesian inference in gravitational-wave astronomy: parameter estimation, model selection, and hierarchical models, *Publ. Astron. Soc. Austral.* **36**, e010 (2019), arXiv:1809.02293 [astro-ph.IM].
- [65] S. R. Taylor and D. Gerosa, Mining gravitational-wave catalogs to understand binary stellar evolution: A new hierarchical Bayesian framework, *Phys. Rev. D* **98**, 083017 (2018), arXiv:1806.08365 [astro-ph.HE].
- [66] B. Abbott *et al.* (LIGO Scientific, Virgo), Binary Black Hole Population Properties Inferred from the First and Second Observing Runs of Advanced LIGO and Advanced Virgo, *Astrophys. J. Lett.* **882**, L24 (2019), arXiv:1811.12940 [astro-ph.HE].
- [67] S. M. Gaebel, J. Veitch, T. Dent, and W. M. Farr, Digging the population of compact binary mergers out of the noise, *MNRAS* **484**, 4008 (2019), arXiv:1809.03815 [astro-ph.IM].
- [68] I. Mandel, W. M. Farr, and J. R. Gair, Extracting distribution parameters from multiple uncertain observations with selection biases, *MNRAS* **486**, 1086 (2019), arXiv:1809.02063 [physics.data-an].
- [69] S. Vitale, One, No One, and One Hundred Thousand – Inferring the properties of a population in presence of selection effects, arXiv e-prints (2020), arXiv:2007.05579 [astro-ph.IM].
- [70] J. Roulet, T. Venumadhav, B. Zackay, L. Dai, and M. Zaldarriaga, Binary Black Hole Mergers from LIGO/Virgo O1 and O2: Population Inference Combining Confident and Marginal Events, arXiv e-prints (2020), arXiv:2008.07014 [astro-ph.HE].
- [71] S. R. Dolan, Instability of the massive Klein-Gordon field on the Kerr spacetime, *Phys. Rev. D* **76**, 084001 (2007), arXiv:0705.2880 [gr-qc].
- [72] S. L. Detweiler, Klein-Gordon equation and rotating black holes, *Phys. Rev. D* **22**, 2323 (1980).
- [73] G. Ficarra, P. Pani, and H. Witek, Impact of multiple modes on the black-hole superradiant instability, *Phys. Rev. D* **99**, 104019 (2019), arXiv:1812.02758 [gr-qc].
- [74] D. Baumann, H. S. Chia, and R. A. Porto, Probing ultralight bosons with binary black holes, *Physical Review D* **99**, 044001 (2019).
- [75] D. Baumann, H. S. Chia, R. A. Porto, and J. Stout, Gravitational Collider Physics, *Phys. Rev. D* **101**, 083019 (2020), arXiv:1912.04932 [gr-qc].
- [76] J. Zhang and H. Yang, Gravitational floating orbits around hairy black holes, *Phys. Rev. D* **99**, 064018 (2019), arXiv:1808.02905 [gr-qc].
- [77] J. Zhang and H. Yang, Dynamic Signatures of Black Hole Binaries with Superradiant Clouds, arXiv e-prints, arXiv:1907.13582 (2019), arXiv:1907.13582 [gr-qc].
- [78] D. Wysocki, J. Lange, and R. O’Shaughnessy, Reconstructing phenomenological distributions of compact binaries via gravitational wave observations, arXiv e-prints, arXiv:1805.06442 (2018), arXiv:1805.06442 [gr-qc].
- [79] B. P. Abbott, R. Abbott, T. D. Abbott, M. R. Abernathy, F. Acernese, K. Ackley, C. Adams, T. Adams, P. Addesso, and R. X. Adhikari, Properties of the Binary Black Hole Merger GW150914, *Phys. Rev. Lett.* **116**, 241102 (2016), arXiv:1602.03840 [gr-qc].
- [80] E. E. Salpeter, The Luminosity function and stellar evolution, *Astrophys. J.* **121**, 161 (1955).
- [81] S. F. Portegies Zwart and S. L. W. McMillan, Black Hole Mergers in the Universe, *Astrophysical Journal Letters* **528**, L17 (2000), astro-ph/9910061.
- [82] M. C. Miller and V. M. Lauburg, Mergers of Stellar-Mass Black Holes in Nuclear Star Clusters, *ApJ* **692**, 917 (2009), arXiv:0804.2783.
- [83] R. M. O’Leary, B. Kocsis, and A. Loeb, Gravitational waves from scattering of stellar-mass black holes in galactic nuclei, *MNRAS* **395**, 2127 (2009), arXiv:0807.2638.
- [84] J. M. B. Downing, M. J. Benacquista, M. Giersz, and R. Spurzem, Compact binaries in star clusters - II. Escapers and detection rates, *MNRAS* **416**, 133 (2011), arXiv:1008.5060.
- [85] B. Kocsis and J. Levin, Repeated bursts from relativistic scattering of compact objects in galactic nuclei, *Phys. Rev. D* **85**, 123005 (2012), arXiv:1109.4170 [astro-ph.CO].
- [86] D. Tsang, Shattering Flares during Close Encounters of Neutron Stars, *ApJ* **777**, 103 (2013), arXiv:1307.3554 [astro-ph.HE].
- [87] B. M. Ziosi, M. Mapelli, M. Branchesi, and G. Tormen, Dynamics of stellar black holes in young star clusters with different metallicities - II. Black hole-black hole binaries, *MNRAS* **441**, 3703 (2014), arXiv:1404.7147.
- [88] C. L. Rodriguez, M. Morscher, B. Pattabiraman, S. Chatterjee, C.-J. Haster, and F. A. Rasio, Binary Black Hole Mergers from Globular Clusters: Implications for Advanced LIGO, *Physical Review Letters* **115**, 051101 (2015), arXiv:1505.00792 [astro-ph.HE].
- [89] C. L. Rodriguez, M. Morscher, B. Pattabiraman, S. Chatterjee, C.-J. Haster, and F. A. Rasio, Erratum: Binary Black Hole Mergers from Globular Clusters: Implications for Advanced LIGO [Phys. Rev. Lett. 115, 051101 (2015)], *Physical Review Letters* **116**, 029901 (2016).
- [90] M. Morscher, B. Pattabiraman, C. Rodriguez, F. A. Rasio, and S. Umbreit, The Dynamical Evolution of Stellar Black Holes in Globular Clusters, *ApJ* **800**, 9 (2015), arXiv:1409.0866.

- [91] M. Dominik, K. Belczynski, C. Fryer, D. E. Holz, E. Berti, T. Bulik, I. Mandel, and R. O’Shaughnessy, Double compact objects. ii. cosmological merger rates, *The Astrophysical Journal* **779**, 72 (2013).
- [92] K. K. Y. Ng, S. Vitale, A. Zimmerman, K. Chatzioannou, D. Gerosa, and C.-J. Haster, Gravitational-wave astrophysics with effective-spin measurements: Asymmetries and selection biases, *Phys. Rev. D* **98**, 083007 (2018), arXiv:1805.03046 [gr-qc].
- [93] S. S. Bavera, T. Fragos, Y. Qin, E. Zapartas, C. J. Neijssel, I. Mandel, A. Batta, S. M. Gaebel, C. Kimball, and S. Stevenson, The origin of spin in binary black holes: Predicting the distributions of the main observables of Advanced LIGO, *Astron. Astrophys.* **635**, A97 (2020), arXiv:1906.12257 [astro-ph.HE].
- [94] L. Barsotti, S. Gras, M. Evans, and P. Fritschel, Updated Advanced LIGO sensitivity design curve, <https://dcc.ligo.org/T1800044-v5/public> (2018), Technical Report LIGO-T1800044-v5.
- [95] B. P. Abbott *et al.*, Prospects for observing and localizing gravitational-wave transients with Advanced LIGO, Advanced Virgo and KAGRA, *Living Reviews in Relativity* **21**, 3 (2018), arXiv:1304.0670 [gr-qc].
- [96] J. Veitch *et al.*, Parameter estimation for compact binaries with ground-based gravitational-wave observations using the LAL-Inference software library, *Phys. Rev. D* **91**, 042003 (2015), arXiv:1409.7215 [gr-qc].
- [97] LIGO Scientific Collaboration, LIGO Algorithm Library - LALSuite, free software (GPL) (2018), <https://git.ligo.org/lscsoft/lalsuite>.
- [98] R. Smith, S. E. Field, K. Blackburn, C.-J. Haster, M. Purrer, V. Raymond, and P. Schmidt, Fast and accurate inference on gravitational waves from precessing compact binaries, *Physical Review D* **94**, 044031 (2016).
- [99] B. F. Schutz, Networks of gravitational wave detectors and three figures of merit, *Class. Quant. Grav.* **28**, 125023 (2011), arXiv:1102.5421 [astro-ph.IM].
- [100] A. Ly, J. Verhagen, and E.-J. Wagenmakers, Harold jeffreys’s default bayes factor hypothesis tests: Explanation, extension, and application in psychology, *Journal of Mathematical Psychology* **72**, 19 (2016).
- [101] M. Vallisneri, J. Kanner, R. Williams, A. Weinstein, and B. Stephens, The LIGO Open Science Center, in *Journal of Physics Conference Series*, Journal of Physics Conference Series, Vol. 610 (2015) p. 012021, <https://www.gw-openscience.org>, arXiv:1410.4839 [gr-qc].
- [102] R. Abbott *et al.* (LIGO Scientific, Virgo), Open data from the first and second observing runs of Advanced LIGO and Advanced Virgo, arXiv e-prints (2019), arXiv:1912.11716 [gr-qc].
- [103] M. Baryakhtar, R. Lasenby, and M. Teo, Black Hole Superradiance Signatures of Ultralight Vectors, *Phys. Rev.* **D96**, 035019 (2017), arXiv:1704.05081 [hep-ph].
- [104] R. Brito, S. Grillo, and P. Pani, Black hole superradiant instability from ultralight spin-2 fields, *Phys. Rev. Lett.* **124**, 211101 (2020), arXiv:2002.04055 [gr-qc].
- [105] M. Dominik, E. Berti, R. O’Shaughnessy, I. Mandel, K. Belczynski, C. Fryer, D. E. Holz, T. Bulik, and F. Pannarale, Double Compact Objects III: Gravitational Wave Detection Rates, *Astrophys. J.* **806**, 263 (2015), arXiv:1405.7016 [astro-ph.HE].
- [106] K. K. Ng, K. W. Wong, T. Broadhurst, and T. G. Li, Precise LIGO Lensing Rate Predictions for Binary Black Holes, *Phys. Rev. D* **97**, 023012 (2018), arXiv:1703.06319 [astro-ph.CO].
- [107] M. Oguri, Effect of gravitational lensing on the distribution of gravitational waves from distant binary black hole mergers, *Mon. Not. Roy. Astron. Soc.* **480**, 3842 (2018), arXiv:1807.02584 [astro-ph.CO].
- [108] V. Baibhav, E. Berti, D. Gerosa, M. Mapelli, N. Giacobbo, Y. Bouffanais, and U. N. Di Carlo, Gravitational-wave detection rates for compact binaries formed in isolation: LIGO/Virgo O3 and beyond, *Phys. Rev.* **D100**, 064060 (2019), arXiv:1906.04197 [gr-qc].
- [109] B. P. Abbott *et al.* (KAGRA, LIGO Scientific, VIRGO), Prospects for Observing and Localizing Gravitational-Wave Transients with Advanced LIGO, Advanced Virgo and KAGRA, *Living Rev. Rel.* **21**, 3 (2018), arXiv:1304.0670 [gr-qc].
- [110] M. Punturo *et al.*, The Einstein Telescope: A third-generation gravitational wave observatory, *Class. Quant. Grav.* **27**, 194002 (2010).
- [111] LIGO Scientific Collaboration, Instrument Science White Paper 2018, <https://dcc.ligo.org/T1800133/public> (2018), Technical Report LIGO-T1800133.
- [112] S. Vitale, W. M. Farr, K. Ng, and C. L. Rodriguez, Measuring the star formation rate with gravitational waves from binary black holes, *Astrophys. J. Lett.* **886**, L1 (2019), arXiv:1808.00901 [astro-ph.HE].
- [113] D. Shoemaker (LIGO Scientific), Gravitational wave astronomy with LIGO and similar detectors in the next decade, arXiv e-prints (2019), arXiv:1904.03187 [gr-qc].
- [114] M. Maggiore *et al.*, Science Case for the Einstein Telescope, *JCAP* **03**, 050, arXiv:1912.02622 [astro-ph.CO].
- [115] D. Reitze *et al.*, Cosmic Explorer: The U.S. Contribution to Gravitational-Wave Astronomy beyond LIGO, *Bull. Am. Astron. Soc.* **51**, 035 (2019), arXiv:1907.04833 [astro-ph.IM].
- [116] R. X. Adhikari *et al.*, Astrophysical science metrics for next-generation gravitational-wave detectors, *Class. Quant. Grav.* **36**, 245010 (2019), arXiv:1905.02842 [astro-ph.HE].
- [117] E. D. Hall and M. Evans, Metrics for next-generation gravitational-wave detectors, *Class. Quant. Grav.* **36**, 225002 (2019), arXiv:1902.09485 [astro-ph.IM].